7452 *Inorg. Chem.* **2010**, *49*, 7452–7463
DOI: 10.1021/ic1007704

Inorganic Chemistry
Article

Vanadium Diaminebis(phenolate) Complexes: Syntheses, Structures, and Reactivity in Sulfoxidation Catalysis

Sónia Barroso, Pedro Adão, Filipe Madeira, M. Teresa Duarte, João Costa Pessoa, and Ana M. Martins*

Centro de Química Estrutural, Instituto Superior Técnico, TU Lisbon, 1049-001 Lisboa, Portugal

Received April 21, 2010

Vanadium diaminebis(phenolate) complexes of the general formulas [LVCl(THF)] (L = $Me_2NCH_2CH(R)N(CH_2$-2-O-3,5-$C_6H_2{}^tBu_2)_2$, where R = H, Me) and [LV(O)X] [X = Cl; R = H (**2**), Me (**3**), O^{i}Pr (**4**), (μ-O)V(O)L (**5**)] are described. All compounds display octahedral geometry and *trans*-O_{Ph} coordination. For compounds **2**, **3**, and **5**, only one isomer, presenting the V═O ligand trans to the tripodal nitrogen, was formed, while for **4**, two isomers were observed by NMR in solution. The UV−vis and circular dichroism spectra of **2** and **3** display very intense charge-transfer transition bands from the phenolate donors to the vanadium, which are in agreement with the ^{51}V low-field shifts observed. All vanadium(V) complexes were tested as thioanisole sulfoxidation catalysts, revealing very high selectivity when H_2O_2 was used as the oxidant. However, no enantioselectivity was observed even when enantiopure **3** was used as the catalyst precursor. ^{1}H and ^{51}V NMR studies were conducted for the reactions of **2** with aqueous solutions of H_2O_2 in methanol-d_4 and in acetonitrile-d_3; **2** reacts with the solvents, leading to [LV(O)OMe], by replacement of Cl by MeO in methanol, and to a new vanadium aminebis(phenolate) complex, where the dimethylamine fragment of the original ligand L was replaced by CH_3CN. In either case, ^{51}V NMR spectra suggest the formation of peroxovanadium species upon the addition of a H_2O_2 solution. The subsequent addition of thioanisole to the methanol-d_4 solution leads to regeneration of the original complex.

Introduction

The roles of vanadium in biological and pharmacological processes are important milestones responsible for the growing interest in the chemistry of vanadium.[1] The importance of high-oxidation-state vanadium complexes is closely related to the catalytic applications of vanadium-dependent haloperoxidases in the halogenation of organic substrates and in selective sulfoxidations.[2] Envisaging modeling or mimicking either the structure or the role of the enzyme active centers,[2i−k] a variety of oxo- and/or peroxovanadium complexes, which are effective catalysts of sulfide oxidation under mild conditions, were reported. Typically, H_2O_2 or organic hydroperoxides are used as oxo-transfer agents. Attempts to elucidate the nature of the active species and the crucial features of the reaction mechanism by NMR and other techniques revealed the presence of several species under catalytic conditions. Additionally, the dynamic behavior of some complexes increases the complexity of the catalytic systems. In spite of this, it is accepted that a side-on-bound hydroperoxo ligand is a requirement for oxygen transfer to the substrate. Protonation may activate the peroxide by enhancing its reactivity, and the reaction is thought to proceed by the direct attack of the substrate to the inner, metal-bound, peroxo oxygen atom.[1c,2k−n]

The synthesis of chiral sulfoxides, mediated by well-defined chiral vanadium catalysts, only reaches regular ee values.[2g,o] A more efficient procedure, which often attains high enantioselectivity, uses in situ generated catalysts, obtained from convenient oxovanadium(IV) or -(V) compounds, a peroxide, and a variable excess of chiral ligand precursors, typically in V:L = 1:1−3.[2h,o] In these conditions,

*To whom correspondence should be addressed. E-mail: ana.martins@ist.utl.pt.

(1) (a) Rehder, D. *Bioinorganic Vanadium Chemistry*; John Wiley & Sons, Ltd.: New York, 2008. (b) Tracey, A. S.; Willsky, G. R.; Takeuchi, E. S. *Chemistry, Biochemistry, Pharmacology and Practical Applications*; CRC Press: Boca Raton, FL, 2007. (c) Ligtenbarg, A. G. J.; Hage, R.; Feringa, B. L. *Coord. Chem. Rev.* **2003**, *237*, 89. (d) Rehder, D.; Santoni, G.; Licini, G. M.; Schulzke, C.; Meier, B. *Coord. Chem. Rev.* **2003**, *237*, 53. (e) Crans, D. C.; Smee, J. J.; Gaidamauskas, E.; Yang, L. *Chem. Rev.* **2004**, *104*, 849.

(2) (a) Hirao, T. *Chem. Rev.* **1997**, *97*, 2707. (b) Smith, T. S.; Pecoraro, V. L. *Inorg. Chem.* **2002**, *41*, 6754. (c) Wu, P.; Çelik, C.; Santoni, G.; Dallery, J.; Rehder, D. *Eur. J. Inorg. Chem.* **2008**, *33*, 5203. (d) Santoni, G.; Rehder, D. *J. Inorg. Biochem.* **2004**, *98*, 758. (e) Schneider, C. J.; Zampella, G.; Greco, C.; Pecoraro, V. L.; Gioia, L. D. *Eur. J. Inorg. Chem.* **2007**, *4*, 515. (f) Wikete, C.; Wu, P.; Zampella, G.; De Gioia, L.; Licini, G.; Rehder, D. *Inorg. Chem.* **2007**, *46*, 196. (g) Lippold, I.; Becher, J.; Klemm, D.; Plass, W. *J. Mol. Catal. A: Chem.* **2009**, *299*, 12. (h) Beller, M.; Bolm, C. *Transition Metals for Organic Synthesis*, 2nd revised and enlarged ed.; Wiley-VCH: Berlin, 2004; Vol. *2*, pp 479−507. (i) Mba, M.; Pontini, M.; Lovat, S.; Zonta, C.; Bernardinelli, G.; Kündig, P. E.; Licini, G. *Inorg. Chem.* **2008**, *47*, 8616. (j) Kravitz, J. Y.; Pecoraro, V. L. *Pure Appl. Chem.* **2005**, *77*, 1595. (k) Zampella, G.; Fantucci, P.; Pecoraro, V. L.; Gioia, L. D. *Inorg. Chem.* **2006**, *45*, 7133. (l) Schneider, C. J.; Penner-Hahn, J. E.; Pecoraro, V. L. *J. Am. Chem. Soc.* **2008**, *130*, 2712. (m) Colpas, G. C.; Hamstra, B. J.; Kampf, J. W.; Pecoraro, V. L. *J. Am. Chem. Soc.* **1996**, *118*, 3469. (n) Balcells, D.; Maseras, F.; Lledós, A. *J. Org. Chem.* **2003**, *68*, 4265. (o) Bolm, C. *Coord. Chem. Rev.* **2003**, *237*, 245.

 Published on Web 07/19/2010

systems derived from Schiff-base frameworks reach very high enantiomeric excess and selectivity toward sulfoxide in the oxidation of particular prochiral substrates.

Vanadium(III) complexes are exceptionally reactive species that enable a remarkable variety of transformations.[3] Its extreme susceptibility to oxidation provides a convenient entry into the chemistry of vanadium(V) that was explored in this work, where we report the syntheses of vanadium(III) and -(V) diaminebis(phenolate) complexes and investigate oxovanadium compounds as catalyst precursors of thianisole sulfoxidation. Diverse amine/phenolate donor sets proved adequate as supporting ligands of a range of early-transition-metal complexes displaying interesting catalytic properties,[4] but, surprisingly, vanadium complexes were scarcely reported,[5] and catalytic applications of vanadium diaminebis(phenolate) compounds in oxidation reactions have not been previously described.

Results and Discussion

Syntheses and Spectroscopic Studies. The synthesis of $Me_2NCH_2CH_2N(CH_2\text{-}2\text{-}HO\text{-}3,5\text{-}C_6H_2{}^tBu_2)_2$ (H_2L^1) was previously reported through a well-established Mannich condensation procedure using as reagents *N*,*N*-dimethylethylenediamine, formaldehyde, and 2,4-di-*tert*-butylphenol.[6] Here we describe a chiral variant of this ligand, $Me_2NCH_2CH(Me)N(CH_2\text{-}2\text{-}HO\text{-}3,5\text{-}C_6H_2{}^tBu_2)_2$ (H_2L^2), which was prepared by an analogous procedure in 60% yield starting from {(*R*)-1-(dimethylamino)-2-propylammonium}{(*R*,*R*)-tart}. The resolution of the commercially available racemic mixture of 1-(dimethylamino)-2-propylamine was carried out using (*R*,*R*)-tartaric acid. {(*R*)-1-(dimethylamino)-2-propylammonium}{(*R*,*R*)-tart} was precipitated out of the solution as a microcrystalline white solid, upon the addition of methanol, in 37% yield. Ligand precursors H_2L^1 and H_2L^2 are shown in Scheme 1.

As depicted in Scheme 2, $VCl_3(THF)_3$ (THF = tetrahydrofuran) is a convenient entry into the synthesis of a series of vanadium diaminebis(phenolate) complexes. [V(L^1)Cl(THF)] (**1**) was obtained in 76% yield as a green crystalline solid upon treatment of $VCl_3(THF)_3$ with 1 equiv of the sodium derivative of the diaminebis(phenolate) ligand precursor Na_2L^1. The magnetic susceptibility of **1** was determined as μ_{eff}(22 °C) = 2.45 μ_B in accordance with its formulation as a d^2 species.

Scheme 1

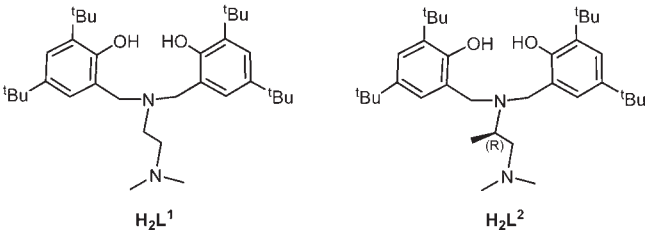

Scheme 2

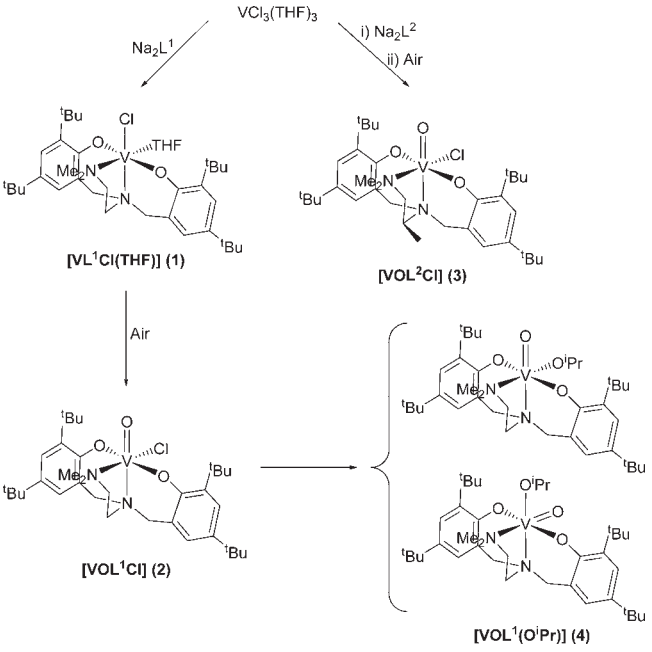

The unequivocal identification of [V(L^1)Cl(THF)] was made by X-ray diffraction analysis of single crystals obtained from Et_2O solutions at −20 °C (see below).

Oxidation of a THF solution of **1** in air led to the formation of a blue solution of [V(L^1)(O)Cl] (**2**), which was isolated in 75% yield. The ^1H and ^{13}C NMR spectra of **2** are compatible with an average C_s symmetry and are consistent with *trans*-phenolate coordination. The methylenic protons bridging the tripodal nitrogen atom and the phenolate rings are diastereotopic and show as one AX system at 4.11 and 3.01 ppm. The two resonances assigned to the methylenic protons of the C_2 chain appear much more shielded than that in the ligand precursor (δ 2.58 ppm in H_2L^1 vs 1.87 and 1.66 ppm in **2**) most possibly as a consequence of the anisotropy caused by the phenolate ring current. The ^{51}V NMR spectrum of **2** displays one broad peak at δ −275.2 ppm in C_6D_6 and at δ −300.8 ppm in $CDCl_3$. The latter value compares well with δ −355 and −366 ppm that were obtained in the same solvent for related oxovanadium aminephenolate complexes.[5a,d]

Treatment of $VCl_3(THF)_3$ with Na_2L^2, followed by in situ oxidation of the vanadium(III) solution with air, led to a chiral complex [V(L^2)(O)Cl] (**3**; Scheme 2) that was isolated from a THF solution in 60% yield as a blue microcrystalline solid. The ^1H and ^{13}C NMR spectra of **3** display C_1 symmetry, as expected. The four methylenic

(3) Janas, Z.; Sobota, P. *Coord. Chem. Rev.* **2005**, *249*, 2144.

(4) (a) Amgoune, A.; Thomas, C. M.; Carpentier, J.-F. *Macromol. Rapid Commun.* **2007**, *28*, 693. (b) Busico, V.; Cipullo, R.; Friederichs, N.; Ronca, S.; Togrou, M. *Macromolecules* **2003**, *36*, 3806. (c) Capacchione, C.; Proto, A.; Ebeling, H.; Mülhaupt, R.; Möller, K.; Spaniol, T. P.; Okuda, J. *J. Am. Chem. Soc.* **2003**, *125*, 4964. (d) Tshuva, E. Y.; Groysman, S.; Goldberg, I.; Goldschmidt, Z. *Organometallics* **2002**, *21*, 662. (e) Gendler, S.; Groysman, S.; Goldschmidt, Z.; Shuster, M.; Kol, M. *J. Polym. Sci., Part A: Polym. Chem.* **2006**, *44*, 1136. (f) Lian, B.; Beckerle, K.; Spaniol, T. P.; Okuda, J. *Eur. J. Inorg. Chem.* **2009**, 311. (g) Amgoune, A.; Thomas, C. M.; Roisnel, T.; Carpentier, J.-F. *Chem.—Eur. J.* **2006**, *12*, 169. (h) Salata, M. R.; Marks, T. J. *J. Am. Chem. Soc.* **2008**, *130*, 12. (i) Liu, X.; Shang, X.; Tang, T.; Hu, N.; Pei, F.; Cui, D.; Chen, X.; Jing, X. *Organometallics* **2007**, *26*, 2747. (j) Gendler, S.; Segal, S.; Goldberg, I.; Goldschmidt, Z.; Kol, M. *Inorg. Chem.* **2006**, *45*, 4783.

(5) (a) Mba, M.; Pontini, M.; Lovat, S.; Zonta, C.; Bernardinelli, G.; Kündig, P. E.; Licini, G. *Inorg. Chem.* **2008**, *47*, 8616. (b) Wolff, F.; Lorber, C.; Choukroun, R.; Donnadieu, B. *Inorg. Chem.* **2003**, *42*, 7839. (c) Lorber, C.; Wolff, F.; Choukroun, R.; Vendier, L. *Eur. J. Inorg. Chem.* **2005**, *14*, 2850. (d) Groysman, S.; Goldberg, I.; Goldschmidt, Z.; Kol, M. *Inorg. Chem.* **2005**, *44*, 5073. (e) Slebodnick, C.; Pecoraro, V. L. *Inorg. Chim. Acta* **1998**, *283*, 37.

(6) Tshuva, E. Y.; Versano, M.; Goldberg, I.; Kol, M.; Weitman, H.; Goldschmidt, Z. *Inorg. Chem. Commun.* **1999**, *2*, 371.

protons of the N(CH_2)Ph moieties appear as two doublets at δ 5.11 and 2.96 ppm and a complex multiplet integrating to two protons at δ 3.15 ppm that results from the overlap of two resonances. The protons directly bonded to the carbons of the C_2 chain spread from δ 2.83 to 1.18 ppm as three resonances integrating 1:1:1. It is pertinent to note that in **3** the resonance assigned to the proton adjacent to the tripodal amine, NC*H*(Me)CH_2NMe_2, is strongly shifted to low field in relation to **2** (δ 2.83 ppm in **3** vs δ 1.66 ppm in **2**). As suggested by the molecular structure of **3** discussed below, this shift is most likely a consequence of the torsion of the C_2 chain caused by the methyl group bonded to the same carbon. As a result, the NC*H*(Me) proton moves away from the shielding influence produced by the phenolate ring current and shows up very close to the chemical shift displayed in the free ligand. In C_6D_6, the ^{51}V NMR resonance of complex **3** appears at δ −257.9 ppm, in accordance with the value observed for **2**.

The addition of 1.5 equiv of LiO^{i}Pr to a toluene solution of **2** led to the synthesis of [V(L^1)(O)O^{i}Pr] (**4**), which was isolated in 40% yield as a mixture of two isomers (Scheme 2). In complex **4a**, the oxo ligand is trans to the tripodal nitrogen, as in **2**, whereas in **4b**, it occupies a cis position in relation to the tripodal nitrogen. The identification of the two isomers was based on the NMR spectra that also revealed that the cis isomer is the major species in solution (**4a**:**4b** = 1:2). In C_6D_6, the ^{51}V NMR spectrum displays two resonances at δ −418.6 and −504.4 ppm assigned to **4a** and **4b**, respectively. The deviation to high field observed in the ^{51}V NMR resonances of **4** when compared to **2** and **3** follows the usual trend taking into account the higher electronegativity of O vs Cl. Indeed, the vanadium chemical shifts were shown to move to high field as the electronegativity of nonpolarizable ligands at vanadium increases.[7] This effect, which is a consequence of stabilization of the highest occupied molecular orbital (HOMO), is accompanied by an increase in the mean HOMO−lowest unoccupied molecular orbital (LUMO) gap and causes a decrease in the paramagnetic shielding term σ_{para} that governs the vanadium chemical shift values.[1a,8a,b]

Treatment, under nitrogen, of an aqueous solution of $VOCl_2$ with H_2L^1 in ethanol (EtOH), followed by neutralization with NaOH, led to a brown solution likely containing a vanadium(IV) diaminebis(phenolate) complex. The solution was exposed to air, resulting in a color change to blue, and after workup, [V(L^1)(O)]$_2$(μ-O) (**5**) was obtained as a blue crystalline solid in 47% yield. The oxidation of vanadium to vanadium(V) is attested to by the ^{1}H and ^{13}C NMR spectra of **5** that display one set of resonances for the diaminebis(phenolate) ligand, consistent with an average C_s symmetry. The ^{1}H NMR spectra did not show resonances other than those of the L^1 ligand, suggesting that a bridging oxo ligand might be linking two [V(L^1)(O)] centers. This hypothesis was confirmed by the single-crystal X-ray determination of **5** as shown below. The ^{51}V NMR spectrum of **5** displays one broad peak at

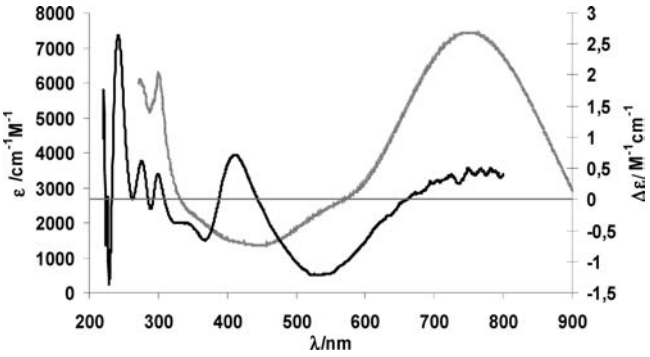

Figure 1. Isotropic absorption (thick line) and CD (thin line) spectra for complex **3** in chloroform. The absorption spectrum was recorded using a 3.21×10^{-4} M solution with a 10 mm optical path cell. The CD spectrum was recorded with a 1.60×10^{-3} M solution with a 1 mm optical path cell.

Table 1. Isotropic Absorption and CD Data for Complex **3**

UV−vis		CD	
λ_{max}/nm	ε/M^{-1} cm^{-1}	λ_{max}/nm	$\Delta\varepsilon$/M^{-1} cm^{-1}
		320	−0.35
360s h	2090	370	−0.65
420 sh	1430	410	+0.72
550 sh	2460	535	−1.21
750	7436	770	+0.47

δ −471.6 ppm in C_6D_6, δ −469.7 ppm in $CDCl_3$, and δ −454.9 ppm in MeOD-d_4.

Globally, complexes **2**−**5** display rather deshielded ^{51}V NMR resonances, resulting from significant delocalization of the electron density toward the metal. In fact, quite low-energy ligand-to-metal charge-transfer (LMCT) transitions are observed in the absorption spectra of complexes **2** and **3** as described next.

The absorption spectra of **2** and **3** are quite similar, as expected, and show remarkable intense bands for $\lambda >$ ca. 500 nm. Figure 1 shows isotropic absorption and circular dichroism (CD) spectra of solutions of complex **3** in chloroform, and Table 1 summarizes the λ_{max} band values and the corresponding ε and $\Delta\varepsilon$ values.

The strong absortivity of the vanadium(V) complexes **2** and **3** is due to LMCT transitions. Rather similarly intense CT transitions from phenolate oxygen atoms to empty d vanadium orbitals have been observed for a few other monooxovanadium(V) phenolates, e.g., V^VO(EHPG), V^VO(EHGS), and V^VO(salen)$^+$,[9a−c] (EHPG = ethylenebis[(*o*-hydroxyphenyl)glycine], EHGS = *N*-[2-(*o*-salicylideneamino)ethyl](*o*-hydroxyphenyl)glycine, salen = *N*,*N*′-disalicylideneethylenediamine), and Bonadies and Carrano[9a] mentioned that there is a correlation between the intensity of these CT bands and the formal charge on the vanadium center, with the highest values corresponding to the highest charge. In the case of complexes **2** and **3**, the CT bands display λ_{max} up to ca. 770 nm at appreciably higher values than those of the referred complexes, for which λ_{max} is about 580 nm and the intensity of the bands is also much higher than those in those complexes. Considering that complexes **2** and **3** present *trans*-phenolate ligands and that in the above-mentioned

(7) Devore, D. D.; Lichtenhan, J. D.; Takusagawa, F.; Maatta, E. A. *J. Am. Chem. Soc.* **1987**, *109*, 7408.
(8) (a) Nakano, T. *Bull. Chem. Soc. Jpn.* **1977**, *50*, 661. (b) Rehder, D. *Inorg. Chem.* **1988**, *27*, 584.
(9) (a) Bonadies, J. A.; Carrano, C. J. *J. Am. Chem. Soc.* **1986**, *108*, 4088. (b) Li, X.; Lah, M. S.; Pecoraro, V. L. *Inorg. Chem.* **1988**, *27*, 4657. (c) Bonadies, J. A.; Butler, W. M.; Pecoraro, V. L.; Carrano, C. J. *Inorg. Chem.* **1987**, *26*, 1218.

Chart 1

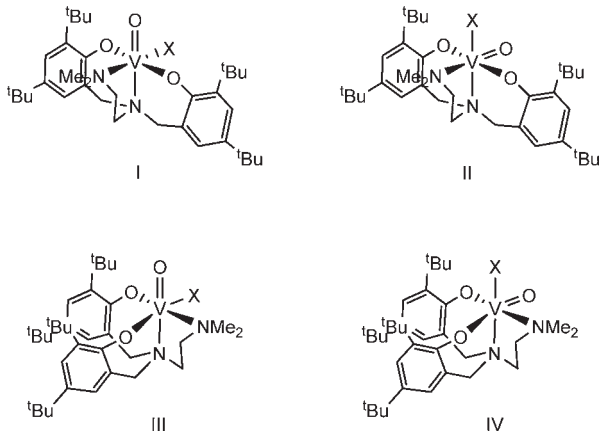

compounds those ligands are cis-coordinated, one might expect that this structural change might be related with the charge at the metal and, thus, might be responsible for significant differences in the corresponding absorption spectra. To assess this issue, the geometries of the various possible isomers of **2**, depicted in Chart 1, have been optimized using the B3LYP/6-31G** level (see below). The results are consistent with the molecular structure obtained by X-ray diffraction because the most stable isomer of **2** has *trans*-O_{Ph} donors. In addition, calculations showed that the net positive charge at the metal is similar in all isomers, making it impossible to establish a direct dependence between the metal charge and the *cis*- or *trans*-phenolate bonding.

It is interesting to note that, although the chiral carbon center is a few bonds away from the aromatic rings, there is a relatively efficient transmission of chirality to the $\pi \rightarrow \pi^*$ transitions, and several CD bands are recorded in the range 230−300 nm; moreover, at least five CD-active transitions are recorded for $\lambda > 300$ nm, probably all CT bands. The dissymmetry factor (df = $\Delta\varepsilon/\varepsilon$) for the transitions are ca. $(3-5) \times 10^{-4}$, much lower than 0.01, the value normally considered for magnetic-dipole-allowed transitions (ca. 10^{-2}),[10a] often found for CT transitions.[10b,c]

Crystallographic Studies. The molecular structure of **1** is shown in Figure 2, and relevant bond lengths and angles are listed in Table 1. The vanadium is bonded to two oxygen and two nitrogen atoms of the diaminebis(phenolate) ligand and to one chloride atom and one oxygen atom of a THF molecule in a distorted octahedral geometry.

The metal ion coordination in **1** is identical with that of the titanium(III) complex [Ti(L^1)Cl(THF)][11] that also displays *trans*-phenolate oxygen atoms and the chloride and the tripodal nitrogen atoms occupying axial trans-bonding positions. On the contrary, complexes **1** and [V{$Me_2NCH_2CH_2N(CH_2$-2-O-3,5-$C_6H_2Me_2)_2$}(Cl)(THF)],[5c] which only differ on the phenolate ring substituents (^{t}Bu in **1** and Me in the latter compound), present different ligand-bonding arrangements. While in **1** the chloride [Cl(1)] and tripodal nitrogen [N(1)] atoms occupy trans coordination positions, in [V{$Me_2NCH_2CH_2N(CH_2$-2-O-3,5-$C_6H_2Me_2)_2$}(Cl)(THF)], those atoms are cis-coordinated. This difference is possibly dictated by the bulkiness of the ^{t}Bu substituents that push away the THF ligand and force it to coordinate trans to N(2). Most likely still reflecting the bulkiness of the ^{t}Bu groups compared to methyl, the coordination angle O(1)−V(1)−O(2) in **1** is slightly shorter than that in [V{$Me_2NCH_2CH_2N(CH_2$-2-O-3,5-$C_6H_2Me_2)_2$}(Cl)(THF)] [165.58(17)° vs 173.90°] and, in contrast, the angles C(11)−O(1)−V(1) and C(21)−O(2)−V(1) in **1** are slightly wider, reflecting the π contribution of the phenolate oxygen atoms to the bonding to vanadium. Despite these differences, the V(1)−X(*i*) bond lengths in both complexes are very similar and comparable to distances observed in other vanadium(III) complexes, namely, [V{$N(CH_2$-2-O-3,5-$C_6H_2{}^tMe_2)_3$}(THF)][5d] and [V{$N(CH_2CH_2NC_6F_5)_3$}(THF)].[12]

ORTEP views of **2** and **3** are shown in Figures 3 and 4, respectively, and selected bond distances and angles are presented in Table 2.

The metal coordination geometry in complexes **2** and **3** is best described as distorted octahedral with the equatorial plane defined by atoms O(1), O(2), N(2), and Cl(1), while

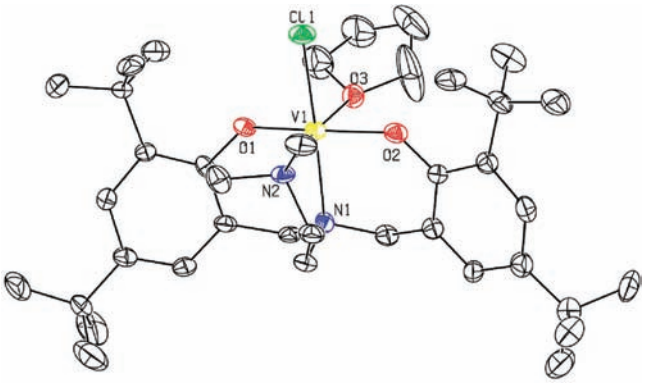

Figure 2. ORTEP diagram of **1** using 40% probability ellipsoids. The hydrogen atoms are omitted for clarity.

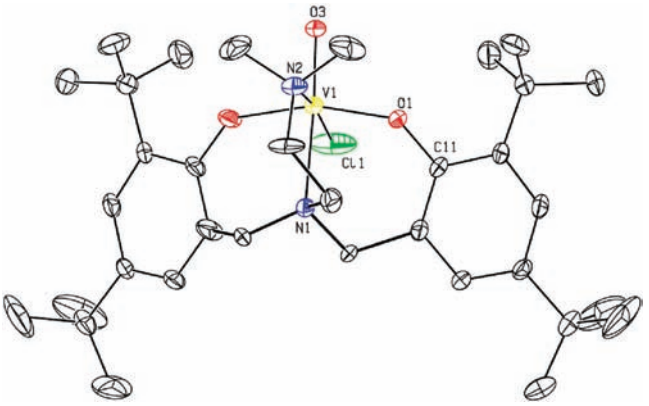

Figure 3. ORTEP diagram of **2** using 40% probability ellipsoids. The hydrogen atoms and disordered carbon atoms are omitted for clarity.

(10) (a) Gillard, R. D. *Prog. Inorg. Chem.* **1966**, *7*, 215. (b) Cavaco, I.; Costa Pessoa, J.; Costa, D.; Duarte, M. T.; Gillard, R. D.; Matias, P. M. *J. Chem. Soc., Dalton Trans.* **1994**, 149. (c) Cavaco, I.; Costa Pessoa, J.; Duarte, M. T.; Henriques, R. T.; Matias, P. M.; Gillard, R. D. *J. Chem. Soc., Dalton Trans.* **1996**, 1989.

(11) Barroso, S.; Cui, J.; Carretas, J. M.; Cruz, A.; Santos, I. C.; Duarte, M. T.; Telo, J. P.; Marques, N.; Martins, A. M. *Organometallics* **2009**, *28*, 3449.

(12) Nomura, K.; Davis, W. M.; Schrock, R. R. *Inorg. Chem.* **1996**, *35*, 3695.

the axial positions are occupied by the oxo ligand O(3) and the tripodal N(1) atom of the diaminebis(phenolate) ligand. In both compounds, the two phenolate moieties of L^1 and L^2 are trans to each other, in agreement with the structures observed in solution by NMR.

We highlight two significant differences between the structures of compounds **2** and **3**: (i) the bending of the phenolate rings and (ii) the conformations of the two six-membered metallacycles. As shown in Figure 5, in complex **2**, the two phenolate moieties bend toward the Cl(1) ligand, defining an angle of 124.1(1)°, while in **3**, the phenolate orientation is the opposite; that is, the two rings bend toward N(2) with an angle of 157.7(1)° between its planes. Furthermore, in **2**, the conformations of the six-membered metallacycles V(1)−N(1)−C(17)−C(16)−C(11)−O(1) and V(1)−N(1)−C(18a)−C(16a)−C(11a)−O(1a) are chair and boat, respectively, whereas in **3**, the two metallacycle conformations are chair.

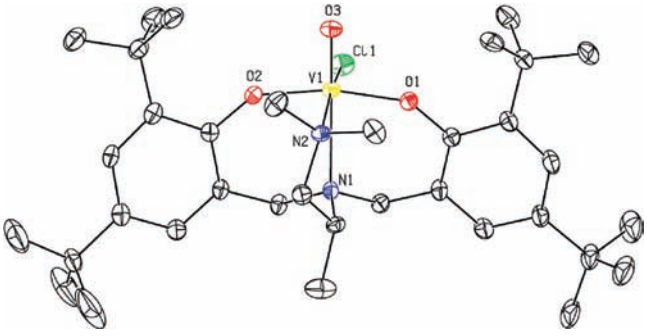

Figure 4. ORTEP diagram of **3** using 40% probability ellipsoids. The hydrogen atoms are omitted for clarity.

On the other hand, the five-membered metallacycles defined by V(1)−N(1)−C(1)−C(2)−N(2) display λ conformation in both compounds (Figure 5). In **3**, this conformation maximizes the separation between the methyl substituent and the phenolate ring that is at the same side of the five-membered metallacycle. In this conformation, the C(1)−C_{Me} bond [C_{Me} = C(5)] nearly bisects the angle between the two phenolate rings. The change in the dihedral angles V(1)−N(1)−C(1)−C(2) in **2** [57.5(5)°] and in **3** [36.8(2)°] reflects the steric constraint imposed by the CH_3 substituent at C(1). The difference between these angles is possibly the cause of the low-field resonance observed for the proton bonded to C(1) in the ^{1}H NMR spectra of **3** because the torsion of the C_2 chain displaces that nucleus from the ring-current influence.

The distances V(1)−X(*i*) between the vanadium atom and atoms N(2), Cl(1), and O(*i*) [O(*i*) = O(1) in **2** and O(1) and O(2) in **3**] in these complexes are closely related. However, the V(1)−O(3) and V(1)−N(1) bonds show significant differences that are intimately related to the differences previously described. Indeed, the V=O bond in **3** is noticeably shorter than that in **2**, while the opposite is observed for V(1)−N(1) bonds.

The angles V(1)−O(*i*)−C(ipso) are wider in **3** [144.34(18)° and 144.16(17)°] than in **2** [135.0(3)°] or in **1** [134.7(4)° and 137.7(3)°]. The difference may reflect stronger vanadium−phenolate bonds in **3** due to more extensive oxygen-to-metal π donation but, as is often observed, this effect is difficult to evaluate from X-ray diffraction data because it does not cause a noticeable variation in the V−O bond lengths.

The molecular structure of **4b** is depicted in Figure 6, and selected bond distances and angles are presented in Table 2. Once more, the vanadium coordination geometry is best

Table 2. Selected Bond Lengths [Å] and Angles (deg) for Compounds **1**−**5**

	1	2	3	4b	5
V(1)−N(1)	2.193(5)	2.340(5)	2.380(2)	2.249(4)	2.326(5)
V(1)−N(2)	2.197(5)	2.213(6)	2.218(2)	2.400(4)	2.360(5)
V(1)−O(1)	1.906(4)	1.831(3)	1.8293(18)	1.900(4)	1.863(4)
V(1)−O(2)	1.913(4)		1.8276(17)	1.917(4)	1.876(4)
V(1)−O(3)	2.191(4)	1.630(4)	1.5893(18)	1.597(3)	1.608(4)
V(1)−O(4)				1.771(4)	1.7934(11)
V(1)−Cl(1)	2.3776(18)	2.326(2)	2.3436(8)		
O(1)−V(1)−O(2)	165.58(17)		166.87(8)	159.10(15)	164.84(17)
O(1)#1−V(1)−O(1)		162.30(18)			
O(1)−V(1)−O(3)	82.68(16)	98.83(9)	96.26(9)	95.70(18)	95.50(18)
O(2)−V(1)−O(3)	83.69(16)		96.78(9)	94.46(18)	94.72(18)
O(4)−V(1)−O(1)				97.63(17)	94.29(13)
O(4)−V(1)−O(2)				96.79(16)	93.83(13)
O(3)−V(1)−O(4)				107.00(17)	105.07(16)
O(1)−V(1)−N(1)	88.16(16)	81.75(9)	82.79(8)	78.32(15)	84.05(16)
O(2)−V(1)−N(1)	88.01(16)		84.20(8)	82.81(14)	83.24(16)
O(3)−V(1)−N(1)	93.63(17)	163.2(2)	165.78(9)	93.91(17)	165.4(2)
O(4)−V(1)−N(1)				159.03(16)	89.47(13)
O(1)−V(1)−N(2)	99.24(17)	91.24(12)	90.20(8)	82.44(15)	83.13(17)
O(2)−V(1)−N(2)	93.79(18)		88.46(8)	84.53(15)	85.73(17)
O(3)−V(1)−N(2)	173.36(17)	91.24(12)	89.25(9)	170.51(17)	89.8(2)
O(4)−V(1)−N(2)				82.49(16)	165.07(13)
N(1)−V(1)−N(2)	80.13(17)	77.01(17)	76.59(8)	76.60(16)	75.65(17)
O(1)−V(1)−Cl(1)	92.43(12)	87.31(11)	88.31(6)		
O(2)−V(1)−Cl(1)	92.64(13)		90.11(6)		
O(3)−V(1)−Cl(1)	91.56(12)	103.50(16)	103.57(7)		
N(1)−V(1)−Cl(1)	174.81(14)	93.31(14)	90.59(6)		
N(2)−V(1)−Cl(1)	94.69(13)	170.32(14)	167.18(6)		
C(11)−O(1)−V(1)	134.7(4)	135.0(3)	144.34(18)	127.0(3)	
C(21)−O(2)−V(1)	137.3(3)		144.16(17)	122.0(3)	

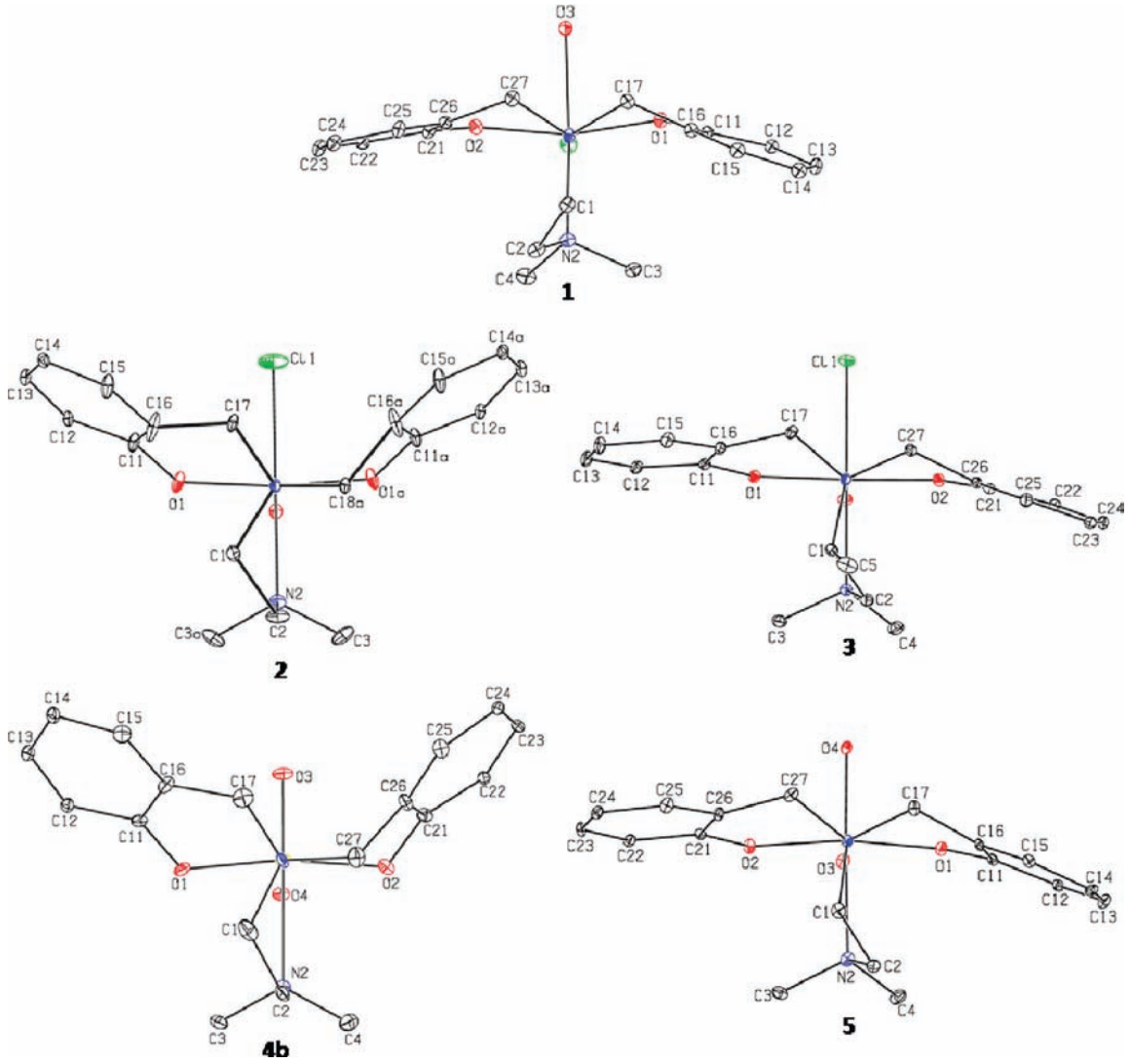

Figure 5. ORTEP partial views of complexes **1**−**5** along the N(1)−V axis using 10% probability ellipsoids.

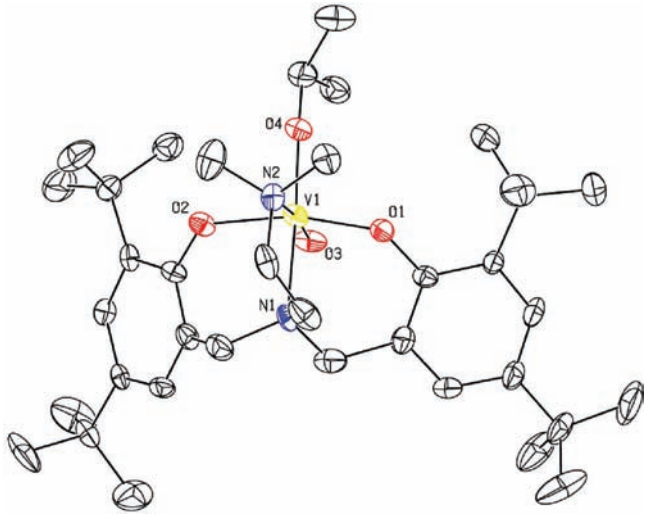

Figure 6. ORTEP diagram of **4** using 40% probability ellipsoids. The hydrogen atoms are omitted for clarity.

described as distorted octahedral, and the equatorial plane is defined by atoms O(1), O(2), N(2), and O(3). The axial positions are occupied by the tripodal nitrogen N(1) and the oxygen of the isopropyl ligand O(4). The V−O bond causes a noticeable distortion in the equatorial plane, as is attested by the atom deviation from the mean plane [0.063(2), 0.062(2), −0.069(2), −0.056(2), and −0.222(2) Å for O(1), O(2), O(3), N(2), and V(1), respectively]. A long V(1)−N(2) distance of 2.400(4) Å reflects the trans effect of the oxo group, as was observed in other complexes.[5b] The $V-O_{phenolate}$ distances are within the values observed for these types of complexes, whereas the V(1)−O(4) distance is shorter but comparable to the same bond length in similar compounds.[5b] The overall coordination of the diaminebis(phenolate) ligand in **4b**, considering the conformations of six- and five-membered metallacycles, is shown in Figure 5 and is analogous to **2**.

The molecular structure of **5** is depicted in Figure 7, and selected bond distances and angles are presented in Table 2. The coordination geometry around the metal is distorted octahedral, with atoms O(1), O(2), N(2), and O(4) defining the equatorial plane. The axial positions are occupied by the tripodal nitrogen atom and the oxo ligand as in compounds **2** and **3**. The distortion of the coordination polyhedron in **5** is less pronounced than that

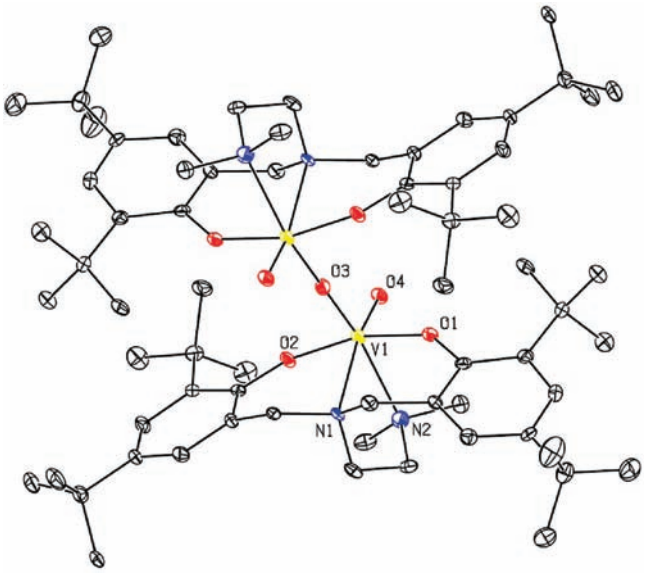

Figure 7. ORTEP diagram of **5** using 40% probability ellipsoids. The hydrogen atoms are omitted for clarity.

in the other vanadium(V) complexes described in this work. The two vanadium centers are linked by a linear V−O−V bridge, with V−O distances in accordance with values observed in other dinuclear oxovanadium complexes. The terminal V=O bond distance is also consistent with the values reported for the other oxovanadium complexes described herein and with other complexes reported in the literature. The V−μ-O−V bond lengths are in accordance with those observed for other vanadium(V) complexes.[13a−e] The coordination of the diaminebis(phenolate) ligand in **5**, considering the conformations of six- and five-membered metallacycles (Figure 5), is similar to that of **3**.

Theoretical Models. The vanadium diaminebis(phenolate) species of the general formula [LV(O)X] with distorted octahedral geometry might, in principle, lead to four different isomers depending on the *cis*- or *trans*-O_{Ph} bonding and on the relative positions of the oxo and X ligands (Chart 1). However, all complexes described in this work display *trans*-phenolate moieties, and the relative positions allowed to the remaining ligands depend on X; if X = Cl (**2** and **3**) or μ-OV(O)L (**5**), only one isomer (I in Chart 1) is observed in solution by NMR, while for X = OR [R = ^{i}Pr, (**4**), Me], two isomers (I and II in Chart 1) are detected. These results may be related to significant energy differences between the various structures and, thus, geometry optimizations of isomers I−IV at the B3LYP/6-31G** level were carried out for complexes **2** and **4**. Simultaneously, the calculations aimed to determine if changes in the ligand coordination may be associated with different metal charges and therefore with LMCT bands.

The calculations have shown that I is the most stable structure for **2**, and considering that the energy differences between I and isomers II−IV are significant (−4.1 kcal mol^{-1} for II, −4.6 kcal mol^{-1} for III, and −9.4 kcal mol^{-1} for IV, respectively), it is not surprising that only one isomer is formed. The calculated and experimental distances and angles, obtained by X-ray diffraction, are in good agreement (Table SI1 in the Supporting Information), and the charge on the vanadium atom in isomers I−IV is essentially the same.

The calculations performed for isomers I and II of complex **4** revealed a small energy difference between the two species. In this case, isomer II is more stable than I by 0.4 kcal mol^{-1}, and it is thus not surprising that the NMR spectra revealed the presence of the two isomers.

Catalytic Studies. The catalytic oxidative ability of the complexes prepared was screened in sulfoxidations using thioanisole as a model compound. An additional objective for the chiral complex **3** was to achieve stereoselective oxidation to the corresponding sulfoxide [(*R*)- or (*S*)-methyl phenyl sulfoxide]. A few control reactions were made to test the lack of thioanisole oxidation by H_2O_2 in the absence of metal and confirm the role of the vanadium complexes as catalysts. The results are presented in Tables 3 and 4.

In 1,2-dichloroethane, the activity of **2** is higher than that of **3** (entries 1 and 4) and within the same order of magnitude of that of **4b** (entries 1 and 11), but the selectivity displayed by all systems is comparable. From the data displayed in Table 3, it may be seen that, in general, relatively small amounts of sulfone are obtained, but no enantioselectivity is achieved when complex **3** was used as a catalyst precursor, regardless of the solvent, temperature, or rate of H_2O_2 addition. Racemic mixtures of the (*R*)- and (*S*)-methyl phenyl sulfoxides are also obtained when the oxidations are carried out with a 1:1.5 ratio of $VO(acac)_2/L^2$, as reported in Table 4. A comparison of the solvents shows that the sulfoxidation is faster in acetone (entry 8 vs entries 3 and 6), and the results also point out that longer reaction times result in higher amounts of sulfone (entries 8 and 9). Thioanisole conversion is proportional to the amount of H_2O_2 (entries 9 and 10), following a 1:1 stoichiometry between the two reagents.

As mentioned above and elsewhere,[2l−n,14] the mechanism of oxidation of thioanisole is normally considered to involve the formation of hydroperoxovanadium(V) complexes. The formation of the hydroperoxo ligand enhances the electrophilicity of the metal-bound oxygen atom, thereby decreasing the activation barrier for the reaction between the peroxide and the sulfur atom. With six-coordinated vanadium(V) complexes, the binding of the peroxide may require the replacement of one of the catalyst precursor donor groups to generate the active species. To check the formation of peroxide complexes in the present systems, ^{1}H and ^{51}V NMR experiments were carried out with complex **2** in methanol-d_4 (Figure 8) and acetonitrile-d_3 (see the Supporting Information) with the addition of H_2O_2.

The dissolution of blue crystals of **2** in methanol-d_4 is accompanied by a drastic color change to brown, and the ^{51}V NMR spectrum shows two resonances (δ −466 and −531 ppm) that disclose the presence of two isomers,

(13) (a) Casellato, U.; Vigato, P. A.; Graziani, R.; Vidali, M.; Milani, F.; Musiani, M. M. *Inorg. Chim. Acta* **1982**, *61*, 121. (b) Chakravarty, J.; Dutta, S.; Chakravorty, A. *J. Chem. Soc., Dalton Trans.* **1993**, 2857. (c) Yamada, S.; Katayama, C.; Tanaka, J.; Tanaka, M. *Inorg. Chem.* **1984**, *23*, 253. (d) Adão, P.; Costa Pessoa, J.; Henriques, R. T.; Kuznetsov, M. L.; Avecilla, F.; Maurya, M. R.; Kumar, U.; Correia, I. *Inorg. Chem.* **2009**, *48*, 3542. (e) Avecilla, F.; Adao, P.; Correia, I.; Costa Pessoa, J. *Pure Appl. Chem.* **2009**, *81*, 1297.

(14) Hamstra, B. J.; Colpas, G. J.; Pecoraro, V. L. *Inorg. Chem.* **1998**, *37*, 949.

Table 3. Sulfoxidation of Thioanisole Using Vanadium Complexes **2**–**5** as Catalyst Precursors

	catalyst	solvent	oxidant[a,b]	*n*(Ox)/*n*(S)	mol % cat.[c]	*T*/°C	*t*/h	convn/%	ee/%	sulfone/%
1	**2**	DCE	H_2O_2	1.2	1	10	18	96	n.d.	11
2	**3**	DCE	H_2O_2	1.2	1	0	40	33	0	1
3	**3**	DCE	H_2O_2	1.2[d]	1	0	24	27	0	1
4	**3**	DCE	H_2O_2	1.2	1	10	36	80	0	9
5	**3**	DCE	H_2O_2	1.2	1	25	4	78	0	3
6	**3**	AcOEt	H_2O_2	1.2	1	0	4	53	0	0
7	**3**	AcOEt	H_2O_2	1.2	1	0	24	84	0	0
8	**3**	$(CH_3)_2CO$	H_2O_2	1.2	1	0	4	>99	0	2
9	**3**	$(CH_3)_2CO$	H_2O_2	1.2	1	0	24	>99	0	9
10	**3**	$(CH_3)_2CO$	H_2O_2	0.5[e]	1	0	24	46	0	0
11	**4b**	DCE	H_2O_2	1.2	2	10	20	93	n.d.	5
12	**4b**	DCE	TBHP[b]	1.2	2	10	20	54	n.d.	0
13	**5**	DCE	H_2O_2	1.2	1	10	20	74	n.d.	14

[a] H_2O_2 20% (w/v) aqueous solution. [b] 5.5 M TBHP in decane. [c] Thioanisole (1 mmol). [d] Added slowly over 3.5 h. [e] Single addition.

Table 4. Sulfoxidation of Thioanisole Using $VO(acac)_2$/L/H_2O_2 Systems[a]

catalyst	*t*/h	convn/%	ee/%	sulfone/%
$VO(acac)_2$[b]	4	34		3
	24	38		11
$VO(acac)_2$/L[1c]	4	79		10
	24	91		14
$VO(acac)_2$/L[2c]	4	89	0	6
	24	91	0	6

[a] Reactions conditions: 1,2-dichloroethane (4 mL), thioanisole (1 mmol), $VO(acac)_2$ (1 mol %), ligand (1.5 mol %, when applicable), and H_2O_2 [1.2 mmol, 30% (w/v) in H_2O] added slowly over 3.5 h, at temperature 0 °C and time 24 h. [b] The aqueous phase acquired a strong yellow color, while the organic phase was colorless. [c] The reaction mixture acquired a deep-brown color after the first drop of oxidant. There was no other change in color during the reaction.

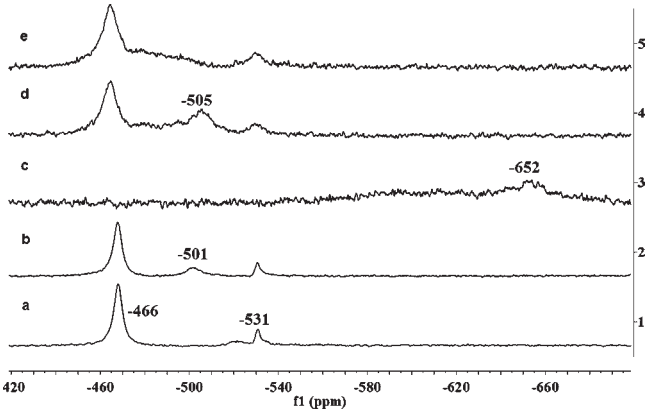

Figure 8. ^{51}V NMR spectra of **2** in MeOD-d_4. ^{51}V NMR spectra of **2** in MeOD-d_4; a) initial spectrum, b) after 0.25 eq. of H_2O_2, c) after 10 eq. of H_2O_2, d) immediately after addition of 10 eq. of thioanisole, e) 24 h later.

identical with **4a** and **4b**, with MeO ligands instead of ^{i}PrO. Upon the addition of 0.25 equiv of a H_2O_2 solution (2.5% in water), a new resonance grows up at δ −501 ppm. All of these signals vanish after the addition of 10 equiv of a H_2O_2 solution, and at this stage, only one ^{51}V NMR resonance is visible at δ −652 ppm. The solution acquired an orange coloration. The ^1H NMR spectrum of this solution is consistent with an average C_s-symmetry species. The benzylic protons adjacent to the tripodal nitrogen atom appear as an AB system (δ, ppm: 4.71, d, $^2J_{HH}$ = 12 Hz, 2H; 4.60, d, $^2J_{HH}$ = 12 Hz, 2H) in agreement with the coordination of the ligand to the vanadium by the two phenolates and the tripodal nitrogen atom. Simultaneously, the C_2 chain and the NMe_2 proton resonances are tentatively assigned to two singlets at δ 3.35 and 3.19 ppm, which might suggest that the dimethylamine moiety is not coordinated to the vanadium. Furthermore, the downfield shift of these resonances is possibly related to the fact that at this pH (ca. 6) the dimethylamine moiety may be protonated. The addition of 10 equiv of thioanisole to the solution gives rise to the disappearance of the high-field resonance and to the immediate reemergence of the signals that were observed after the first addition of a H_2O_2 solution that displays the two original resonances assigned to the [V(L^1)(O)OMe] isomers and a third signal at δ −505 ppm. This signal disappears after 24 h, and the original oxo complexes are regenerated. The solution color turns back to brown.

Even considering that the catalytic reactions are carried out in a heterogeneous medium and the NMR experiment was performed in a homogeneous solution, it may be assumed that the species formed are the same.[15] The assignment of the new vanadium resonances formed immediately after the addition of H_2O_2 is uncertain. It may tentatively be suggested that the signal at δ −505 ppm corresponds to an oxoperoxovanadium species. This type of complex was suggested to participate in the oxidation of thioethers,[16] and their chemical shifts typically range between δ −500 and −600 ppm when supported by N,O-donor ligands.[17] Yet, the small variation in the vanadium chemical shift in relation to the starting complexes may not exclude other possibilities such as, for instance, the hydrolysis of the MeO−V bond. The resonance at δ −652 ppm observed at higher H_2O_2 concentration is not far from the values reported for inorganic diperoxovanadium solutions.[18] This attribution is not consistent with our results because the ^1H NMR spectrum of this sample reveals that the ancillary ligand remains coordinated to the vanadium and the starting complexes are reformed after the addition of thioanisole. In any case, it looks apparent that the new vanadium species formed after the H_2O_2 addition are consumed upon thioanisole

(15) Blum, S. A.; Bergman, R. G.; Ellman, J. A. *J. Org. Chem.* **2003**, *68*, 150.
(16) Bryliakov, K. P.; Karpyshev, N. N.; Fominsky, S. A.; Tolstikov, A. G.; Talsi, E. P. *J. Mol. Catal. A: Chem.* **2001**, *171*, 73.
(17) Karpyshev, N. N.; Yakovleva, O. D.; Talsi, E. P.; Bryliakov, K. P.; Tolstikova, O. V.; Tolstikov, A. G. *J. Mol. Catal. A: Chem.* **2000**, *157*, 91.
(18) Blum, S. A.; Bergman, R. G.; Ellman, J. A. *J. Org. Chem.* **2003**, *68*, 150.

Chart 2

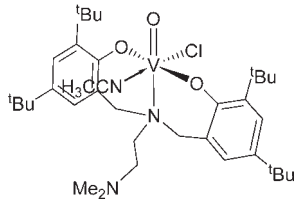

addition, and thus it is likely that both compounds may be involved in substrate oxidation.

Following the dissolution of complex **2** in wet acetonitrile-d_3, a sharp and minor resonance at δ −360 ppm and a broad peak at δ −239 ppm are visible. The high-field resonance is assigned to a residual amount of **2**, and the low-field signal evidences the formation of a new diamagnetic species. The ^{1}H NMR spectrum of this complex suggests the replacement of the dimethylamine moiety by acetonitrile, as shown in Chart 2. The NMR pattern is consistent with a C_s-symmetry complex with two ^{t}Bu singlets (δ 1.54 and 1.29 ppm), two aromatic CH resonances (δ 7.31 and 7.03 ppm), one AB system for the benzylic protons (δ 4.01 and 3.79 ppm; $^2J_{HH}$ = 14.7 Hz), one singlet for the dimethylamine protons (δ 3.01 ppm), two multiplets for the C_2 chain methylenic protons (δ 2.85 and 2.64 ppm), and one broad signal at δ 2.10 ppm assigned to coordinated acetonitrile.

The stepwise addition of an aqueous solution of H_2O_2 (5% w/v) causes vanishing of the initial ^{51}V NMR resonances upon the addition of 5 equiv of H_2O_2. Simultaneously, a new peak starts to build up at δ −608 ppm because of the first addition of H_2O_2; this resonance increases in intensity and very slightly shifts to high field up to δ −613 ppm when 5 equiv of peroxide is added. The addition of H_2O_2 is accompanied by the formation of a small amount of an orange/brownish precipitate and a green solution. At this stage, the ^{1}H NMR spectrum does not allow the identification of any compound, and the vanadium resonance may be compatible with either a peroxovanadium complex or an inorganic peroxovanadate.[2b,5a,e] After the solution stands for 48 h, the ^{51}V NMR spectrum reveals that no diamagnetic species are kept in solution.

Concluding Remarks

Chiral and achiral vanadium(III) and -(V) complexes bearing tripodal diaminebis(phenolate) ligands are described. All complexes display distorted octahedral geometry with *trans*-phenolate ligands. The oxovanadium(V) complexes are very selective toward sulfoxide when used as catalyst precursors for the oxidation of thioanisole. The catalytic reaction is faster when carried out in acetone with H_2O_2 as an oxidant. The reactivity of **2** with aqueous H_2O_2 solutions strongly depends on the solvent and the amount of oxidant. In methanol-d_4, the ^{1}H NMR data suggest the formation of one vanadium species that maintains the two phenolate moieties and the tripodal nitrogen atom bonded to the vanadium, but the dimethylamine is apparently protonated and not coordinated to the metal center. The ^{51}V NMR spectrum indicates the formation of one peroxovanadium species upon the addition of H_2O_2, and the subsequent addition of thioanisole to the NMR solution regenerates the starting complex. The dissolution of **2** in acetonitrile-d_3 leads to the formation of a new complex by replacement of the dimethylamine fragment by acetonitrile. The addition of H_2O_2 gives rise to the appearance of one major vanadium resonance that suggests the formation of a peroxovanadium species, but the ^{1}H NMR data obtained after H_2O_2 addition are inconclusive. As reported for other systems described in the literature, no enantioselectivity is achieved when complex **3** is used as a catalyst precursor, regardless of the solvent, temperature, or rate of H_2O_2 addition. Racemic mixtures of the (*R*)- and (*S*)-methylphenyl sulfoxides are also obtained when the oxidations are carried out with a 1:1.5 ratio of VO(acac)$_2$/L^2.

Experimental Section

General Procedures. Unless otherwise stated, all preparations and subsequent manipulations were carried out using standard Schlenk-line and drybox techniques in an atmosphere of dinitrogen. THF, toluene, pentane, and *n*-hexane were dried by standard methods and degassed prior to use. Toluene-d_8 and benzene-d_6 were dried over sodium and distilled. All other reagents were obtained from commercial sources and used as received. The diaminebis(phenolate) ligand precursor H_2L[16] and $VCl_3(THF)_3$[19] were prepared by literature procedures. 1D (^{1}H, ^{13}C{^{1}H}, and ^{51}V) and 2D NMR spectra were recorded with Bruker Avance II+ 300 and 400 MHz (UltraShield Magnet) spectrometers at ambient temperature. ^{1}H and ^{13}C chemical shifts (δ) are expressed in ppm relative to Me_4Si, and ^{51}V is referenced to external neat $VOCl_3$. The magnetic susceptibility was determined for powdered samples of the compounds using a Sherwood Scientific magnetic susceptibility balance based on the Evans method. Diamagnetic corrections for the diaminebis(phenolate) ligand were applied. Elemental analyses were carried out using a CE Instruments EA110 automatic analyzer. Analysis of the products in sulfoxidations was done by high-performance liquid chromatography (HPLC) (Jasco system: two Intelligent 880-PU HPLC pumps, a two-line degasser 880-51, an Intelligent 870-UV UV−vis detector), using a Rheodyne 725i injector (5 μL), a Daicel Chiralpak IA column, and a Borwing software.

Resolution of Racemic 1-(Dimethylamino)-2-propylamine. The resolution of racemic 1-(dimethylamino)-2-propylamine was carried out with modification of a method described in the literature.[20]1-(Dimethylamino)-2-propylamine (2 mL, 15 mmol) was dissolved in water (3.5 mL) and heated to 80 °C. First (*R*,*R*)-tartaric acid (1.16 g, 7.7 mmol) and then glacial acetic acid (0.75 mL, 13 mmol) were added in small portions with stirring until the pH was close to 6. The mixture was cooled in ice with continued stirring, and methanol was added until a precipitate appeared. The solution was filtered off, and the precipitate was washed with ice-cold methanol and dried in vacuo. Yield: 1.39 g (37%) of white {(*R*)-1-(dimethylamino)-2-propylammonium}{(*R*,*R*)-tart}.

H_2L^2. A solution of {(*R*)-1-(dimethylamino)-2-propylammonium}{(*R*,*R*)-tart} (0.76 g, 3 mmol) in methanol (5 mL) was heated to 80 °C, and K_2CO_3 (0.42 g, 3 mmol) was added. A solution of 2,4-di-*tert*-butylphenol (1.24 g, 6 mmol) and 36% aqueous formaldehyde (0.67 mL, 8.4 mmol) in methanol (10 mL) was then added. The mixture was stirred under reflux for 3 days. The reaction mixture was cooled to room temperature and left overnight in the freezer at −20 °C, leading to a precipitate that was separated by filtration and dried in vacuum. The solid was extracted in Et_2O and filtered, and the solvent was removed under vacuum to give H_2L^2

(19) Manzer, L. E. *Inorg. Synth.* **1982**, *21*, 135.
(20) Galsbøl, F.; Steenbøl, P.; Sørensen, B. S. *Acta Chem. Scand.* **1972**, *26*, 3605.

as a white solid (0.97 g, 60% yield). ^{1}H NMR (δ, ppm, C_6D_6): 7.50 (s, 2H, Ar), 6.98 (s, 2H, Ar), 3.91 (d, J_{HH} = 12.4 Hz, 2H, NCH_2Ar), 2.93 (m, 3H, NCH_2Ar + NCH(CH$_3$)CH$_2$N), 2.14 (m, 1H, NCH(CH$_3$)CH_2N), 1.96 (s, 6H, N(CH_3)$_2$), 1.67 (s, 18H, C(CH_3)$_3$), 1.45 (m, 1H, NCH(CH$_3$)CH_2N), 1.36 (s, 18H, C-(CH_3)$_3$)), 0.54 (d, J_{HH} = 6.2 Hz, 3H, NCH(CH_3)CH$_2$N). ^{13}C{^{1}H} NMR (δ, ppm, C_6D_6): 153.9, 140.6, 136.5, 125.4 (*ipso*-Ar), 123.6 and 122.3 (Ar), 81.8 (NCH(CH$_3$)CH$_2$N), 61.8 (ArCH$_2$N), 61.8 (NCH(CH$_3$)CH$_2$N), 48.7 (N(CH$_3$)$_2$), 35.5 and 34.3 (C(CH$_3$)$_3$), 32.0 and 30.1 (C(CH$_3$)$_3$), 8.48 (NCH(CH$_3$)CH$_2$N). Elem. anal. Calcd for $C_{35}H_{58}N_2O_2\cdot 0.5CH_4O$: C, 76.8; H, 10.9; N, 5.0. Found: C, 77.2; H, 11.3; N, 5.1.

[V(L^1)Cl(THF)] (1). A solution of H_2L^1 (1.02 g, 2 mmol) in THF was slowly added to NaH (0.106 g, 4.40 mmol), and the mixture was stirred for 1.5 h at room temperature. The colorless solution of Na_2L^1 was filtered through a Celite layer and added to a suspension of $VCl_3(THF)_3$ (0.723 g, 2 mmol) in THF at −30 °C. The temperature was allowed to rise slowly to room temperature, and the solution was further stirred for 4 h. The green solution obtained was filtered and evaporated to dryness, leading to **1** as a green crystalline solid in 76% yield (0.984 g, 1.48 mmol). Crystals suitable for X-ray diffraction were obtained from Et_2O at −20 °C. μ_{eff} (20 °C) = 2.45 μ_B. Elem. anal. Calcd for $C_{38}H_{62}ClN_2O_3V\cdot 0.5C_4H_8O$: C, 67.0; H, 9.2; N, 4.1. Found: C, 62.3; H, 8.5; N, 4.0 (elemental analysis results reflect the extreme instability of the compound in air).

[V(L^1)(O)Cl] (2). A solution of H_2L^1 (2.704 g, 5 mmol) in THF was slowly added to NaH (0.264 g, 11 mmol), and the mixture was stirred for 1.5 h at room temperature. The colorless solution of Na_2L was filtered through a Celite layer and added to a suspension of $VCl_3(THF)_3$ (1.807 g, 5 mmol) in THF at −30 °C. The temperature was allowed to rise slowly, and the solution was stirred for 4 h at room temperature. The green solution was exposed to air for 18 h, leading to a blue solution that was filtered and evaporated to dryness. [V(L^1)(O)Cl] was obtained as a blue crystalline solid in 75% yield (0.90 g, 1.44 mmol). Blue crystals suitable for X-ray diffraction were obtained from a THF solution at room temperature, by the slow evaporation of the solvent at atmospheric pressure. ^{1}H NMR (δ, ppm, C_6D_6): 7.56 (d, 2H, J_{HH} = 2.26 Hz, Ar), 6.95 (d, 2H, J_{HH} = 2.19 Hz, Ar), 4.11 (d, 2H, J_{HH} = 14.09 Hz, NCH_2Ar), 3.01 (d, 2H, J_{HH} = 14.16 Hz, NCH_2Ar), 2.40 (s, 6H, N(CH_3)$_2$), 1.87 (m, 2H, NCH$_2$CH_2N(CH$_3$)$_2$)), 1.83 (s, 18H, C(CH_3)$_3$), 1.66 (m, 2H, NCH_2CH$_2$N(CH$_3$)$_2$)), 1.35 (s, 18H, C(CH_3)$_3$). ^{13}C{^{1}H} NMR (δ, ppm, C_6D_6): 166.9, 145.9, 135.9, and 127.7 (*ipso*-Ar), 124.6 and 123.6 (Ar), 63.0 (NCH$_2$Ar), 58.8 (NCH$_2$$CH_2$N(CH$_3$)$_2$)), 53.3 (N($CH_3$)$_2$), 52.5 (N$CH_2CH_2$N(CH$_3$)$_2$)), 36.3 and 35.1 ($C$(CH$_3$)$_3$), 32.2 (C($CH_3$)$_3$), 31.6 (C($CH_3$)$_3$). ^{51}V NMR ($\delta$, ppm): −275.2 ($C_6D_6$), −300.8 ($CDCl_3$). FT-IR (KBr, cm^{-1}): ν(V=O) 958. Elem. anal. Calcd for $C_{34}H_{54}ClN_2O_3V\cdot 2H_2O$: C, 61.8; H, 8.8; N, 4.2. Found: C, 61.6; H, 9.1; N, 3.9.

[V(L^2)(O)Cl] (3). A solution of H_2L^2 (2.704 g, 5 mmol) in THF was slowly added to NaH (0.264 g, 11 mmol), and the solution was stirred for 1.5 h at room temperature, leading to a colorless solution of Na_2L^2 that was filtered through Celite and added to a suspension of $VCl_3(THF)_3$ (1.807 g, 5 mmol) in THF at −30 °C. The temperature of the mixture was allowed to rise slowly, and the solution was stirred for a further 6 h at room temperature. The green solution was then exposed to air for 18 h, resulting in a dark-blue solution that was filtered and evaporated to dryness to give [V(L^2)(O)Cl] as a blue crystalline solid in 60% yield (1.92 g, 3 mmol). Blue crystals suitable for X-ray diffraction were obtained from pentane at room temperature. ^{1}H NMR (δ, ppm, C_6D_6): 7.44 (d, 1H, J_{HH} = 1.8 Hz, Ar), 7.50 (d, 1H, J_{HH} = 1.3 Hz, Ar), 6.99 (d, 1H, J_{HH} = 1.4 Hz, Ar), 6.88 (s, 1H, Ar), 5.11 (d, 1H, J_{HH} = 14.6 Hz, NCH_2Ar), 3.15 (m, 2H, NCH_2Ar), 2.96 (d, 1H, J_{HH} = 13.8 Hz, NCH_2Ar), 2.83 (br, 1H, NCH(CH$_3$)CH$_2$N), 2.68 (s, 3H, N(CH_3)$_2$), 2.35 (s, 3H, N(CH_3)$_2$), 2.09 (t, 1H, J_{HH} = 13.0 Hz, NCH(CH$_3$)CH_2N), 1.88 (s, 9H, C(CH_3)$_3$), 1.78 (s, 9H, C(CH_3)$_3$), 1.37 (s, 9H, C(CH_3)$_3$), 1.30 (s, 9H, C(CH_3)$_3$), 1.18 (s, 1H, NCH(CH$_3$)-CH_2N), 0.29 (d, J_{HH} = 4.9 Hz, NCH(CH_3)CH$_2$N) . ^{13}C{^{1}H} NMR (δ, ppm, C_6D_6): 168.6, 164.9, 146.4, 144.9, 136.4, 133.9, 127.4, 127.2 (*ipso*-Ar), 124.6, 124.2, 123.5, and 122.9 (Ar), 64.2 (NCH(CH$_3$)CH$_2$N), 59.5 (NCH$_2$Ar), 54.4 (NCH$_2$Ar), 54.3 and 52.7 (N(CH$_3$)$_2$), 52.6 (NCH(CH$_3$)CH$_2$N), 34.8 and 34.7 (C(CH$_3$)$_3$), 31.9, 31.7, 31.3, and 31.2 (C(CH$_3$)$_3$), 7.8 (NCH(CH$_3$)CH$_2$N). ^{51}V NMR (δ, ppm, C_6D_6): −257.9. FT-IR (KBr, cm^{-1}): ν(V=O) 954. Elem. anal. Calcd for $C_{35}H_{56}ClN_2O_3V$: C, 65.8; H, 8.8; N, 4.4. Found: C, 65.4; H, 9.3; N, 4.1.

[V(L^1)(O)O^{i}Pr] (4). A solution of LiO^{i}Pr (0.099 g, 1.5 mmol) and [V(L^1)(O)Cl] (0.874 g, 1.4 mmol) in toluene was stirred for 18 h at room temperature, leading to a dark-purple solution. The solvent was evaporated to dryness, and the residue was extracted in hexane and filtered off. Evaporation of hexane to dryness led to a brown solid identified as [V(L^1)(O)O^{i}Pr] in 32% yield (0.350 g, 0.54 mmol). NMR experiments revealed a mixture of *trans*-[V(L^1)(O)O^{i}Pr] (**4a**) and *cis*-[V(L^1)(O)O^{i}Pr] (**4b**) isomers in a ratio of 1:2. **4a**. ^{1}H NMR (δ, ppm, C_6D_6): 7.50 (d, 2H, J_{HH} = 2.3 Hz, Ar), 7.00 (d, 2H, J_{HH} = 2.3 Hz, Ar), 5.25 (sept, J_{HH} = 6.1 Hz, 1H, CH(CH$_3$)$_2$), 3.85 (d, 2H, J_{HH} = 13.8 Hz, NCH_2Ar), 3.26 (d, 2H, J_{HH} = 13.8 Hz, NCH_2Ar), 2.65 (s, 6H, N(CH_3)$_2$), 2.01 (m, 2H, NCH_2CH$_2$NMe$_2$), 1.94 (m, 2H, NCH$_2$CH_2NMe$_2$), 1.83 (s, 18H, C(CH_3)$_3$), 1.38 (s, 18H, C(CH_3)$_3$), 0.83 (d, J_{HH} = 6.1 Hz, 6H, CH(CH_3)$_2$). ^{13}C{^{1}H} NMR (δ, ppm, C_6D_6): 166.0, 141.2, 134.0, and 125.1 (*ipso*-Ar), 123.6 and 122.7 (Ar), 84.0 (CH(CH$_3$)$_2$), 62.0 (NCH$_2$Ar), 57.7 (NCH$_2$$CH_2NMe_2$), 55.9 (N$CH_2CH_2NMe_2$), 52.0 (N($CH_3$)$_2$), 35.57 and 34.39 ($C$(CH$_3$)$_3$), 31.99 (C($CH_3$)$_3$), 31.15 (C($CH_3$)$_3$), 24.8 (C($CH_3$)$_2$). ^{51}V NMR ($\delta$, ppm, C_6D_6): −418.6. **4b**. ^{1}H NMR (δ, ppm, C_6D_6): 7.60 (d, 2H, J_{HH} = 2.3 Hz, Ar), 7.04 (d, 2H, J_{HH} = 2.1 Hz, Ar), 5.76 (sept, J_{HH} = 5.9 Hz, 1H, CH(CH$_3$)$_2$), 3.98 (d, 2H, J_{HH} = 13.6 Hz, NCH_2Ar), 3.51 (d, 2H, J_{HH} = 13.6 Hz, NCH_2Ar), 2.34 (s, 6H, N(CH_3)$_2$), 2.15 (m, 2H, NCH_2CH$_2$NMe$_2$), 1.99 (m, 2H, NCH$_2$CH_2NMe$_2$), 1.72 (s, 18H, C(CH_3)$_3$), 1.61 (d, J_{HH} = 6.1 Hz, 6H, CH(CH_3)$_2$), 1.41 (s, 18H, C(CH_3)$_3$). ^{13}C{^{1}H} NMR (δ, ppm, C_6D_6): 164.3, 140.7, 135.1, and 125.1 (*ipso*-Ar), 123.4 and 123.2 (Ar), 83.2 (CH(CH$_3$)$_2$) 63.2 (NCH$_2$Ar), 55.1 (NCH$_2$CH$_2$NMe$_2$), 51.9 (NCH$_2$$CH_2NMe_2$), 49.1 (N($CH_3$)$_2$), 35.63 and 34.41 ($C$(CH$_3$)$_3$), 32.04 (C($CH_3$)$_3$), 31.26 (C($CH_3$)$_3$), 25.4 (C($CH_3$)$_2$). ^{51}V NMR ($\delta$, ppm, C_6D_6): −504.4. Crystals of **4b** suitable for X-ray diffraction were obtained from pentane at 4 °C. Elem. anal. Calcd for $C_{37}H_{61}N_2O_4V$: C, 68.5; H, 9.5; N, 4.3. Found: C, 68.3; H, 9.4; N, 3.8.

[V(L^1)(O)]$_2$(μ-O) (5). H_2L^2 (2.26 g, 4.3 mmol) in EtOH was added to a 48.5% (w/v) aqueous solution of $VOCl_2\cdot 2H_2O$ (1.54 mL, 4.3 mmol), and the mixture was stirred for 0.5 h at room temperature, leading to a green solution. The addition of a solution of 1 M NaOH in water until pH ∼8 led to the formation of a brown precipitate that was separated by filtration. The solid was dissolved in Et_2O and exposed to air, leading to a blue solution. Upon evaporation of the solvent, [V(L^1)(O)]$_2$(μ-O) was obtained as a blue crystalline solid in 47% yield (1.2 g, 1 mmol). Blue crystals suitable for X-ray diffraction were obtained from Et_2O at room temperature. ^{1}H NMR (δ, ppm, C_6D_6): 7.50 (d, 4H, J_{HH} = 2.3 Hz, Ar), 6.99 (d, 4H, J_{HH} = 2.2 Hz, Ar), 3.41 (s, 8H, NCH_2Ar), 2.21 (t, 4H, J_{HH} = 5.8 Hz, NCH_2CH$_2$NMe$_2$), 1.94 (m, 4H, NCH$_2$CH_2NMe$_2$ + s, 12H, N(CH_3)$_2$), 1.67 (s, 36H, C(CH_3)$_3$), 1.35 (s, 36H, C(CH_3)$_3$). ^{13}C{^{1}H} NMR (δ, ppm, C_6D_6): 154.3, 141.0, 137.0 (*ipso*-Ar), 125.5, 124.0, and 122.8 (Ar), 57.1 (NCH$_2$Ar), 55.9 (NCH$_2$-CH$_2$NMe$_2$), 49.5 (NCH$_2$$CH_2NMe_2$), 44.9 (N($CH_3$)$_2$), 35.8 and 34.6 ($C$(CH$_3$)$_3$), 32.4 and 30.41 (C($CH_3$)$_2$). ^{51}V NMR ($\delta$, ppm): −470.2 ($C_6D_6$), −454.9 (MeOD-$d_4$), −469.7 ($CDCl_3$). Elem. anal. Calcd for $C_{68}H_{108}N_4O_7V_2\cdot 3.5C_7H_8$: C, 73.2; H, 9.0; N, 3.7. Found: C, 73.3; H, 9.0; N, 4.4.

Table 5. Experimental Crystal Data and Structure Refinement Parameters for Compounds **1**−**5**

	1	**2**	**3**	**4b**	**5**
empirical formula	$C_{38}H_{62}ClN_2O_3V \cdot C_4H_{10}O$	$C_{34}H_{48}ClN_2O_3V$	$C_{35}H_{56}ClN_2O_3V$	$C_{37}H_{61}N_2O_4V$	$C_{68}H_{108}N_4O_7V_2 \cdot C_4H_{10}O$
fw	755.41	619.13	639.21	648.82	1269.58
temperature (K)	150(2)	293(2)	150(2)	293(2)	150(2)
cryst syst	monoclinic	orthorhombic	monoclinic	orthorhombic	triclinic
space group	*P*2/*c*	*Pnma*	*P*21	*Pbca*	$P\bar{1}$
a (Å)	27.851(7)	10.6570(13)	8.7600(4)	18.793(13)	11.5810(18)
b (Å)	9.717(3)	29.284(4)	13.4810(7)	12.942(9)	16.401(3)
c (Å)	17.162(5)	11.3750(11)	15.6210(8)	30.753(5)	20.171(3)
α (deg)	90	90	90	90	75.332(8)
β (deg)	94.182(15)	90	97.534(3)	90	89.037(8)
γ (deg)	90	90	90	90	89.870(8)
V (Å^3)	4632(2)	3549.9(7)	1828.81(16)	7480(7)	3705.9(10)
Z, D_{calcd} (g cm^{-3})	4, 1.083	4, 1.158	2, 1.161	8, 1.152	2, 1.138
μ (mm^{-1})	0.309	0.387	0.378	0.303	0.304
reflns measd	63 105	16 693	32 702	68 709	38 464
unique reflns [*R*(int)]	8293 [0.1852]	3284 [0.0828]	6482 [0.0579]	6663 [0.3785]	12987 [0.1491]
obsd reflns [$I > 2\sigma(I)$]	4324	2141	5645	2398	5306
R1	0.1693	0.1185	0.0493	0.2563	0.2226
wR2	0.2668	0.2270	0.0852	0.1790	0.2563

Solution Sulfoxidation of Thioanisole. The catalytic experiments were carried out at atmospheric pressure, at a constant temperature, in a glass batch reactor, equipped with a magnetic stirrer, a thermometer, and a condenser. In a typical run, the solid catalyst (1 or 2 mol %) and thioanisole (1 mmol) were dissolved in dichloroethane (4 mL). Then the oxidant (1.1 mmol), H_2O_2 (20 wt % aqueous solution) or TBHP (5.5 M in decane), was added to the mixture under stirring. Blank experiments were carried out in the absence of catalyst. Samples of the reaction mixture were withdrawn periodically and analyzed on a Jasco HPLC system equipped with a Daicel Chiralpak IA column. The eluent used was hexane/ethyl acetate (60:40) with a flow of 1 mL min^{-1}. The calibration curves for each reagent and product, namely, sulfide, sulfoxide, and sulfone, were determined using similar HPLC procedures, and these calibrations were used for quantitative analyses. Diphenyl sulfone was used as an internal standard.[13d]

General Procedures for X-ray Crystallography. Crystallographic data for compounds **1**−**5** were collected using graphite-monochromated Mo Kα (α = 0.710 73 Å) on a Bruker AXS-KAPPA APEX II area detector diffractometer equipped with an Oxford Cryosystem open-flow nitrogen cryostat. Cell parameters were retrieved using Bruker *SMART* software and refined using Bruker *SAINT* software on all observed reflections. Absorption corrections were applied using *SADABS*. The structures were solved by direct methods using either *SHELXS-97*[21] or *SIR-97*[22] and refined using full-matrix least-squares refinement against F^2 using *SHELXL-97*.[23] All programs are included in the package of programs *WINGX*, version 1.64.05.[24] All non-hydrogen atoms were refined anisotropically, and the hydrogen atoms were inserted in idealized positions. The molecular diagrams were drawn with *ORTEP3* for Windows,[25] included in the software package. Crystallographic data for **1**−**5** are presented in Table 5.

Green crystals of **1** were obtained from Et_2O at −20 °C. The unit cell contains one molecule and one cocrystallized Et_2O molecule. A second disordered Et_2O molecule was removed using the *SQUEEZE*[26] option in the program *PLATON*.[27] Blue crystals of **2** were obtained from a THF solution at room temperature. The crystals had low quality and poor diffracting power, presenting strong disorder between two conformations with a 50:50% probability around a symmetry plane containing atoms V(1), N(1), N(2), Cl(1), O(3), and C(2). Only one of the conformations is present in the ORTEP drawing for clarity. All non-hydrogen atoms were refined anisotropically, and all hydrogen atoms were placed in idealized positions and allowed to refine by riding on the parent carbon atom [except for C(1), C(2), and C(17) because of the disorder around those atoms].

Blue crystals of **3** were obtained from pentane at room temperature, and data were collected at 150 K. Blue crystals of **4b** were obtained from pentane at 4 °C; they are of low quality and present poor diffracting power, allowing refinement to convergence. Blue crystals of **5** were obtained from an Et_2O solution at room temperature. The unit cell contains two half-molecules and one cocrystallized Et_2O molecule.

Data for compounds **1**−**3**, **4b**, and **5** were deposited with the CCDC under deposit numbers CCDC 772650−772654, respectively, and can be obtained free of charge from the Cambridge Crystallographic Data Center, 12 Union Road, Cambridge CB2 1EZ, U.K. (tel +44 1223 336408, fax +44 1223 336033).

Computational Details. The calculations were performed using the *Gaussian 03* software package[28] and the B3LYP functional, without symmetry constraints, which includes a mixture of Hartree−Fock[29] exchange with the density functional theory[30] exchange correlation, given by Becke's three-parameter functional[31] with the Lee, Yang, and Parr correlation functional (including both local and nonlocal terms[32,33]). The optimized geometries were obtained with a standard 6-31G**[34] basis set for all elements.

Acknowledgment. The authors are grateful to Fundação para a Ciência e a Tecnologia, Portugal, POCI 2010, FEDER,

(21) Sheldrick, G. M. *Acta Crystallogr.* **1990**, *A46*, 467.
(22) Altomare, A.; Burla, M. C.; Camalli, M.; Cascarano, G. L.; Giacovazzo, C.; Guagliardi, A.; Moliterni, A. G. G.; Polidori, G.; Spagna, R. *J. Appl. Crystallogr.* **1999**, *32*, 115.
(23) Sheldrick, G. M. *SHELXL-97, A computer program for refinement of crystal structures*; University of Göttingen: Göttingen, Germany, 1997.
(24) Farrugia, L. J. *J. Appl. Crystallogr.* **1999**, *32*, 837.
(25) Farrugia, L. J. *J. Appl. Crystallogr.* **1997**, *30*, 565.
(26) Sluis, P. v. d.; Spek, A. L. *Acta Crystallogr.* **1990**, *A46*, 194.
(27) Spek, A. L. *Acta Crystallogr.* **1990**, *A46*, C34.
(28) Black, D. G.; Swenson, D. C.; Jordan, R. F.; Rogers, R. D. *Organometallics* **1995**, *14*, 3539.
(29) Hehre, W. J.; Radom, L.; Schleyer, P. v. R.; Pople, J. A. *Ab Initio Molecular Orbital Theory*; John Wiley & Sons: New York, 1986.
(30) Parr, R. G.; Yang, W. *Density Functional Theory of Atoms and Molecules*; Oxford University Press: New York, 1989.
(31) Becke, A. D. *J. Chem. Phys.* **1993**, *98*, 5648.
(32) Lee, C.; Yang, W.; Parr, R. G. *Phys. Rev. B* **1988**, *37*, 785.
(33) Miehlich, B.; Savin, A.; Stoll, H.; Preuss, H. *Chem. Phys. Lett.* **1989**, *157*, 200.
(34) (a) Ditchfield, R.; Hehre, W. J.; Pople, J. A. *J. Chem. Phys.* **1971**, *54*, 724. (b) Hehre, W. J.; Ditchfield, R.; Pople, J. A. *J. Chem. Phys.* **1972**, *56*, 2257. (c) Hariharan, P. C.; Pople, J. A. *Mol. Phys.* **1974**, *27*, 209. (d) Gordon, M. S. *Chem. Phys. Lett.* **1980**, *76*, 163. (e) Hariharan, P. C.; Pople, J. A. *Theor. Chim. Acta* **1973**, *28*, 213.

for funding (research project PTDC/QUI/66187/2006 and fellowships SFRH/BD/28762/2006 and SFRH/BD/40279/2007) and to the Portuguese NMR Network (IST-UTL Centre) for providing access to the NMR facility. The authors thank Prof. Luis Veiros for helping with the geometry optimization of compounds **2** and **4**.

Supporting Information Available: Selected ^{51}V and ^{1}H NMR spectra in CD_3CN and methanol-d_4 with the addition of an aqueous solution of H_2O_2, tables with atomic coordinates of optimized isomers of **2** and **4**, and X-ray crystallographic data for compounds **1**−**5** in CIF format. This material is available free of charge via the Internet at http://pubs.acs.org.